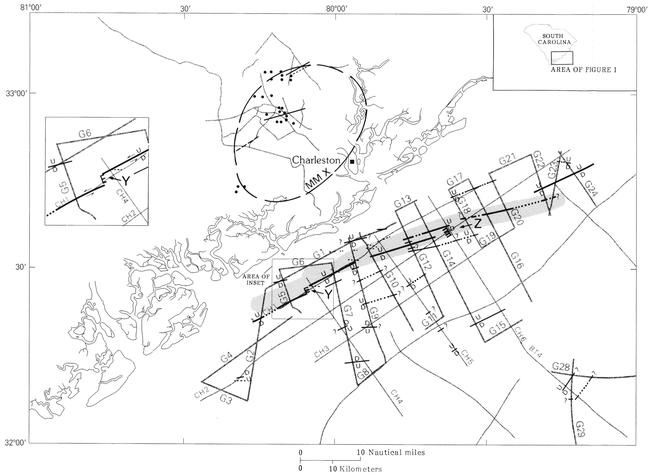

EXPLANATION

- Cenozoic compressional faults--U, upthrown side; D, downthrown side; dotted where projected between known fault segments; queried where existence is uncertain
- U/D ·····? Helena Banks fault
- U/D ·····? Other fault
- Cenozoic normal fault--Hachures on downdropped side
- Cretaceous fault
- Triassic(?) extensional fault
- Epicenter of earthquake detected between March 1973 and December 1979, as reported by Tarr and Rhea (1983)
- *RV Gyre* seismic-reflection tracklines
- Other seismic lines

Figure 1.--Map showing localities of multichannel seismic-reflection profiles offshore and on land in the meizoseismal area and vicinity of the 1886 Charleston earthquake. The tracklines of the high-resolution profiles (G1-G24) and two of the deep-penetration profiles (G28 and G29) collected by the RV Gyre are shown. Tracklines of deep-penetration profiles from an earlier (1979) survey are labelled CH_1; the trackline labelled BT4 is from a 1975 survey and is not discussed here. Some unlabelled seismic lines, from other surveys, are shown. Interpreted Cenozoic (compressional and extensional) and Triassic(?) (extensional) faults are indicated. Cenozoic normal faults Y and Z are interpreted from tracklines CH1 and CH2 respectively. The modified-Mercalli intensity-X isoseismal line for the 1886 earthquake (labelled MM X) is shown from Bollinger (1977). The Helena Banks fault zone overlies the narrow Kiawah Triassic(?) basin, shown by the screen pattern. The faults indicated near the crossing of tracklines G28 and G29 are not discussed in the text but this feature, observed in older data shown by Dillon and others (1979), was discussed by Behrendt and others (1983). Inset shows enlargement of transition area between two main branches of the Helena Banks fault; note normal fault Y perpendicular to the main Helena Banks fault trend from CH1. Paired arrows indicate strike-slip movement.

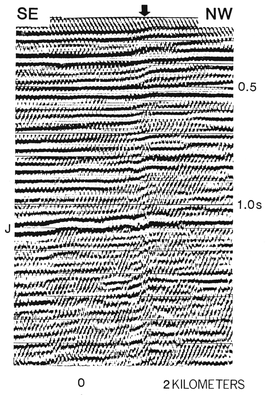

Figure 2.--Section of seismic profile from CH4 crossing the Helena Banks fault (indicated by arrow). J reflection is labelled. Vertical axis is two-way traveltime, in seconds. Vertical exaggeration x6.

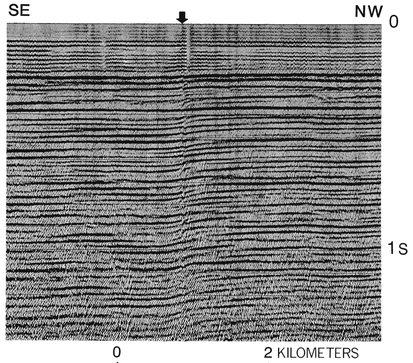

Figure 4.--Seismic section crossing the Helena Banks fault from line G9, plotted at 3:1 vertical exaggeration to show deformation detail. Arrow indicates fault. Vertical axis is two-way traveltime, in seconds.

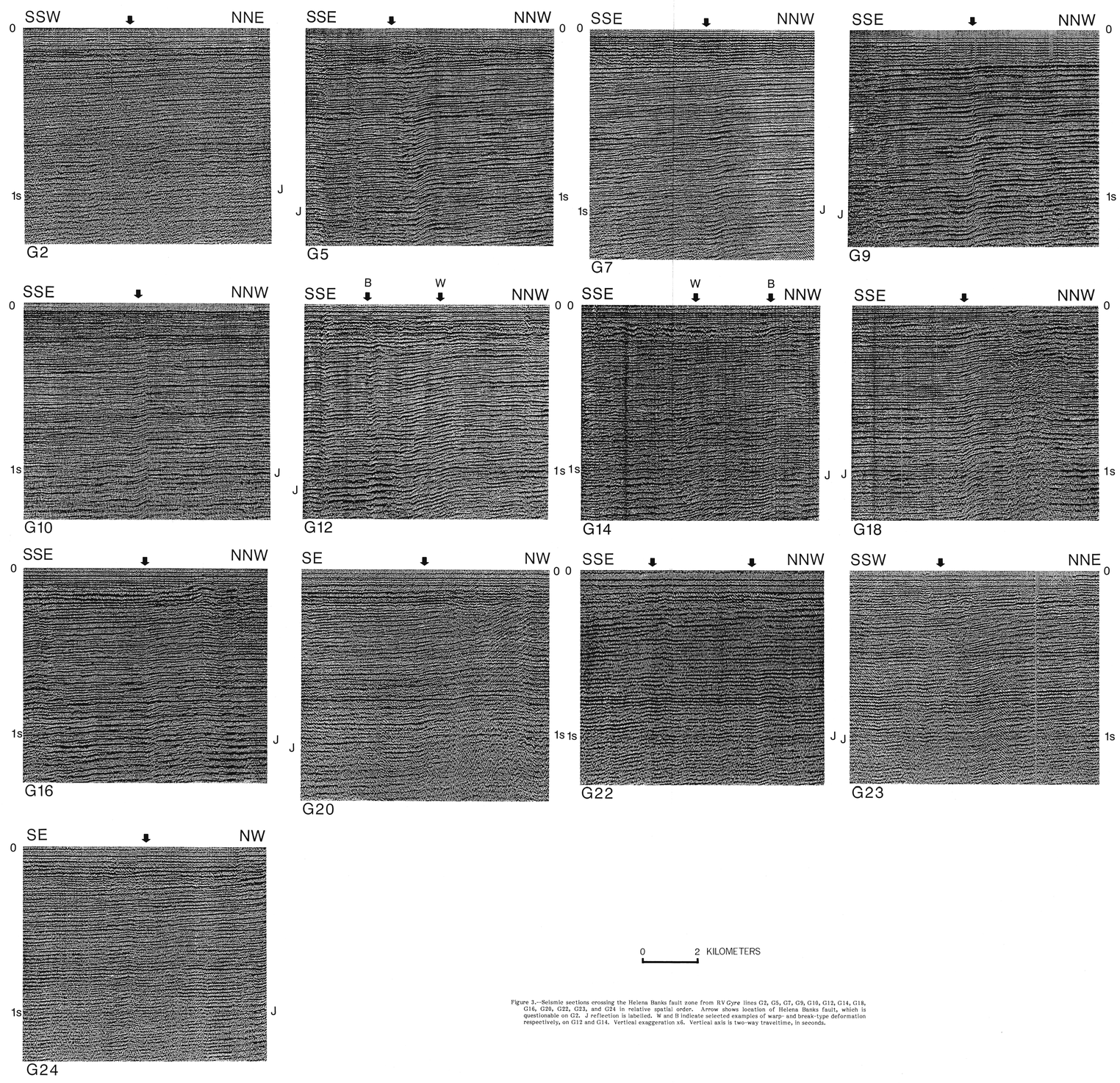

Figure 3.--Seismic sections crossing the Helena Banks fault zone from RV Gyre lines G2, G5, G7, G9, G10, G12, G14, G18, G16, G20, G22, G23, and G24 in relative spatial order. Arrow shows location of Helena Banks fault, which is questionable on G2. J reflection is labelled. W and B indicate selected examples of warp- and break-type deformation respectively, on G12 and G14. Vertical exaggeration x6. Vertical axis is two-way traveltime, in seconds.

Introduction

Since the early 1970's, the U.S. Geological Survey (USGS) has been carrying out integrated seismological, geophysical, and geological studies of the meizoseismal area (area of maximum destructive force) of the Charleston, S.C., earthquake of 1886 and in the surrounding region (fig. 1). Results of some of these studies have been published (for example, Rankin, 1977; Gohn, 1983). The objectives have been to determine the cause of the 1886 earthquake and to evaluate the potential for similar earthquakes in the future there and elsewhere along the U.S. Atlantic seaboard. Although there is no general agreement about the source of the 1886 earthquake, a number of hypotheses have been postulated (summarized by Dewey, 1985).

In 1979 the USGS contracted both land and marine multichannel seismic-reflection profiles to be shot in the Charleston area. The Whitehall Corporation collected the marine data referred to as the CH lines (fig. 1). The shooting parameters of the CH survey allowed sampling of a large area to a depth of 12 seconds (s) (all times given are two-way traveltime). Using these data, Behrendt and others (1981, 1983) defined the northeast-trending Helena Banks fault (see figure 1, lines CH1, CH4, and CH5). Although many of the gross structures and reflectors were mapped, the large common-depth-point spacing tended to obscure the finer structural and stratigraphic details of the profiles. Figure 2 shows an example from the CH data set. Single-channel seismic-reflection profiles showed deformation as shallow as 10 m below the sea bottom. Seismicity has not been observed along the Helena Banks fault or anywhere in the offshore Charleston area (Dewey, 1983; Tarr and Rhea, 1983), but earlier studies concluded that movement along this fault could be the cause of a future large, damaging earthquake (Behrendt and others, 1983; Dewey, 1985; Behrendt and Yuan, 1986, 1987).

In October 1981, a marine geophysical survey was conducted off Charleston by the research vessel (RV) *Gyre*. The objective of the survey was to better define the configuration and history of the Helena Banks fault zone. Three distinct data sets were collected during the *Gyre* cruise: a high-resolution seismic-reflection survey, a deeper-penetration (6-s record length) seismic-reflection survey, and a simultaneous gravity survey. *Gyre* lines 1 through 24 (G1-G24, fig. 1) represent the first high-resolution seismic survey in the offshore Charleston area and are the primary focus of this report. The deep-penetration lines, *Gyre* lines 25 through 29 (only G28 and G29 are shown in figure 1), were located to investigate deep (3 to 5 s) diffractions that were identified on some of the seismic profiles as possible intrusives suggested by previous aeromagnetic studies (Klitgord and Behrendt, 1977, 1979; Behrendt and Klitgord, 1979) and gravity studies (Grow and others, 1979). Gravity data were collected along all the *Gyre* lines although results from lines 27 through 29 are unuseable due to an equipment malfunction. Only the high-resolution data are presented here. Behrendt and Yuan (1986, 1987) discussed these results and their tectonic implications but presented only a few small-scale examples of the actual seismic-reflection record sections.

RV *Gyre* data set

During the seven-day RV *Gyre* cruise, 600 km of high-resolution multichannel seismic-reflection data were collected with a 10-m shotpoint interval and 20-m group interval; an additional 18 km of single-channel minisparker data were obtained over *Gyre* line 12 (G12). The high-resolution *Gyre* lines 1 through 24 combined with the previous CH data provide a dense grid of multichannel seismic-reflection data close to the 1886 meizoseismal area (fig. 1), the densest set of publicly available multichannel seismic-reflection data on the U.S. Atlantic continental margin.

This map shows sections of all the high-resolution seismic-reflection profiles that cross the Helena Banks fault zone (fig. 3). All the sections but one are displayed at a 6:1 vertical exaggeration to enhance the resolution of small-displacement, steeply dipping faults and to match the display of the CH lines. The exception, a section shown in figure 4, has a 3:1 vertical exaggeration. Vertical exaggeration was calculated assuming an average seismic velocity of 2.0 km/s (Behrendt and others, 1983) for the upper second of section, one second corresponding to one kilometer of depth.

Field operations and data processing

The sound source for the high-resolution survey was a tuned array of two 1.3-liter (80-cubic-inch) water guns firing on distance every 10 m. The twelve-channel, 220-m-long streamer had a near offset of 103 m. Using a Texas Instruments DFS V recording system, three seconds of digital data were obtained at a 1-ms sampling rate. However, the higher frequencies were attenuated and this high sample rate was unnecessary. The RV *Gyre* was equipped with an integrated navigation system which combined hyperbolic loran-C with periodic corrections of absolute positions from navigation satellites. The absolute accuracy is estimated to be ± 50 m. The relative error for shotpoints is approximately ± 0.5 m based on position checks made every hundred shotpoints. Such high relative accuracy is important in multichannel processing because in order for multiple traces from different shots to "see" the same depth point, a constant shotpoint interval must be maintained. Common-depth-point traces are then sorted and stacked, enhancing signal and attenuating noise.

The data were processed by means of the USGS seismic-processing system in Denver, Colo. A total of 210 field tapes were demultiplexed and corrected for spherical divergence. Near-trace plots provided a preliminary check on the data. The data were then sorted by common depth point according to the observers' reports, and some editing of bad records was done. Although three seconds of data were recorded in the field, only the first two seconds were processed because of noise at depths below 1.4 s.

Eight common depth points were selected every 1 to 4 km, depending on the uniformity of the strata, for velocity analyses. Three methods of velocity analysis were applied: computer-determined signal coherence versus stacking velocity, constant-velocity analysis applied to stacks, and constant-velocity analysis applied to common-depth-point gathers. Time-velocity pairs that were similar, though independently derived from the three methods, were plotted by common depth point to check for realistic velocity structure. The optimal time-velocity pairs were ultimately stored and used for normal moveout correction. The normal moveout correction accounts for different reflection arrival times due to variations in the offset distance between source and geophone.

The velocity studies from the *Gyre* data show high coherency when gradually increasing stacking velocities (in the 1.7 to 2.0 km/s range) are applied down to the arrival of the J reflection, a significant marker that occurs between 0.8 and 1.2 s throughout the *Gyre* survey area (Behrendt and others, 1983; Behrendt and Yuan, 1986, 1987). The J reflection, which has been identified previously on land (Yantis and others, 1983; Schilt and others, 1983; Hamilton and others, 1983) and offshore (Dillon and others, 1979; Behrendt and others, 1983) and attributed to the high acoustic-impedance contrast between a series of Jurassic (Langhere, 1983) basalt flows and overlying Upper Cretaceous sediments, provided an easily recognized target for processing tests. The lithology and geochemistry of the basalt are discussed by Gohn and others (1977, 1978), Gottfried and others (1977, 1983), and Schneider and others (1979).

Stacking velocities above the J reflection increase with depth gradually, but at the J reflection show a sharp step-like increase of 0.1 to 0.5 km/s; stacking velocities are 2.0-2.5 km/s at depths consistent with the arrival of the J reflection as extrapolated from the CH survey (for example, figure 2). This increase commonly results in a dramatic increase in interval velocities from approximately 1.8-2.0 km/s above the J reflection to 3.0-5.5 km/s at and below the J reflection. The interval velocity range for the J reflection is low when compared to that of the seismic-refraction velocities on land of 4.4 to 5.7 km/s (Ackermann, 1983) and at sea of 5.8 to 6.3 km/s (Dillon and others, 1979). However, these calculated interval velocities are used only to give an indication that stacking velocities used during processing are realistic and consistent with existing information. Velocity analysis below the J reflection proved meaningless due to the poor signal-to-noise ratio and little normal moveout with the short streamer, so a standard stacking velocity of 3.5 km/s at 2.0 s was applied.

Signal analysis included autocorrelation and frequency spectral analysis. We performed standard tests of different deconvolution and bandpass filters, and automatic-gain control gates. Inspection of data from each line determined the severity of the mute (partial seismic-trace editing) and the need for further (whole-trace) editing.

The processing scheme that produced the best results on test sections was applied to the entire seismic profile. For most of the profiles this optimal processing scheme varied little. Typically, the steps used to produce the final stacks were: demultiplex and spherical divergence correction, zero-amplitude shot edit, geometry definition, CDP sort, zero-amplitude channel edit, mute, automatic-gain control (1.0-s gate), predictive (15-ms gap) deconvolution, velocity analysis, time-velocity pairs storage, normal moveout correction, mute, 12-fold stack, bandpass filter (usually 20 to 85 Hz), automatic-gain control (1.0-s gate), and final display. The final stacks in figure 3 were plotted with a horizontal scale of 80 traces per inch and a vertical scale of 7.5 in./s prior to reducing the figure for publication. This high vertical-exaggeration compressed display is unique because all processed traces are included in a high trace-density plot.

After all the final stacks were inspected, specific areas of interest (for example, crossing the Helena Banks fault zone) were selected for reprocessing and display at a more expanded horizontal scale to make full use of the high-density data. The reprocessing involved rigorous velocity analyses, frequent determination of mutes to apply to the common-depth-point gathers after normal moveout correction, application of a time-variant bandpass filter with a lower high-cut (60 to 70 Hz) at and below the arrival of the J reflection, and application of a shorter (500 ms) automatic-gain control gate just before display at 3:1 vertical exaggeration. These expanded-scale sections (for example, figure 4; Behrendt and Yuan, 1987) were helpful in measuring actual displacements and the apparent reverse dip along the Helena Banks fault. The complexities of the fault zone are more apparent on the expanded sections, although the fault is not as obvious as in the compressed display sections.

We migrated only those sections where signal-to-noise ratios were high and the Helena Banks fault was well defined, as in profile G9. Migration failed to improve the seismic appearance of the fault, which indicates that the reflectors involved are relatively smooth and shallow dipping; therefore, we do not include any migrated examples here. Diffractions are not apparent in the Helena Banks fault zone, probably because the unconsolidated Coastal Plain sediments seen in the reflection data are only warped or draped over actual breaks (which would cause diffractions) in the deeper crystalline rocks at and below the J reflector.

The vertical multiple reflection time is 0.027 s for a water depth of 20 m (typical in the Helena Banks fault zone). The first hundred milliseconds of the profiles shown in figure 3 have a "ringing" or reverberating appearance because of the persistent bottom-multiple problem and shallow water depth. However, because of the great offset relative to water depth and the general similarity in appearance of these profiles to those from the same area published previously (Behrendt and others, 1981, 1983), we believe the water-bottom multiple reflections later than about 0.1 s have been effectively removed by deconvolution and stacking.

Helena Banks fault zone

The Helena Banks fault zone is probably a reactivated fault zone that bounds the narrow Kiawah Triassic(?) basin as defined by aeromagnetic and deep-penetration seismic data (Behrendt and Yuan, 1986, 1987; Behrendt and Grim, 1983; Behrendt and Klitgord, 1979; Behrendt and others, 1983). We were able to define in detail the configuration and character of the fault zone from new profiles provided by the *Gyre* survey (Behrendt and Yuan, 1986, 1987). Twelve of these profiles actually cross the fault zone and one, G2, probably crosses the southwest end of the fault zone because reflection evidence for the Helena Banks fault there is obscure. Parts of each of the high-resolution seismic-reflection profiles that cross the fault zone (G2 through G24) are shown here in relative spatial order, from southwest to northeast (fig. 3). Originally defined as one continuous reverse fault (Behrendt and others, 1981, 1983), the Helena Banks fault is now interpreted to be more complex--actually a strike-slip zone, that is approximately 110 km in length and 15 km in width, and is 5 km or more offshore, striking (as a zone) N. 66° E., roughly parallel to the coastline (Behrendt and Yuan, 1986, 1987). The fault zone comprises at least five en echelon 11- to 30-km-long fault segments striking N. 62° E. to N. 77° E.

On final-stacked sections crossing the Helena Banks fault zone from lines G5, G7, G9, G10, G18, G16, and G20 (fig. 3), the fault plane is well defined and reflections are measurably offset. Where G12 and G14 cross the fault zone, we observe several examples of alternating warp and break types of deformation of reflectors instead of one distinct fault.

The seismic profiles from lines G22, G23, and G24 that cross the fault zone show poorly defined fault planes that gently warp the reflectors.

Near the southwestern end of the surveyed area (fig. 1), the seismic sections from lines G5, CH1, and more questionably G2 (fig. 3) define the southwestermost fault segment of the Helena Banks fault. The main segment of the Helena Banks fault is offset slightly to the north of this southwestern segment by 2 km. Apparent reverse faults crossing lines G7, G9, G10, G12, and G14 can be connected with fault locations mapped earlier from lines CH1, CH2, CH4, CH5, and CH6. Two other similarly trending faults can be drawn from locations on lines G12, G14, G16, G18, and CH2; and G18, G16, G20, G22, G23, and CH6. Another fault segment is also offset approximately 4 km to the north and connects locations mapped from lines G22, G23, and G24. We infer that the Helena Banks fault zone is limited to the area between lines G2 and G24.

Although on seismic sections the apparent movement along the Helena Banks fault is reverse faulting contemporaneous with deposition of Coastal Plain sediments, purely reverse motion is unlikely given the northeast orientation of the maximum horizontal compressive stress (Zoback and others, 1986) and the pre-existing fault geometry. A ratio of as much as 10:1 strike-slip to reverse movement is compatible with the magnetic data (Behrendt and Yuan, 1987). The existence of one, possibly two, normal faults perpendicular to the Helena Banks fault trend and connecting the individual fault segments (fig. 1, normal faults Y and Z) supports the interpretation that the Helena Banks fault is a strike-slip fault.

References cited

Ackermann, H.D., 1983, Seismic-refraction study in the area of the Charleston, South Carolina, 1886 earthquake, *in* Gohn, G.S., ed., Studies related to the Charleston, South Carolina, earthquake of 1886--Tectonics and seismicity: U.S. Geological Survey Professional Paper 1313-F, p. F1-F20.

Behrendt, J.C., and Grim, M.S., 1983, Structural elements of the U.S. Atlantic margin delineated by second vertical derivative of aeromagnetic data: U.S. Geological Survey Geophysical Investigations Map GP-956, scale 1:2,500,000.

Behrendt, J.C., Hamilton, R.M., Ackermann, H.D., and Henry, V.J., 1981, Cenozoic faulting in the vicinity of the Charleston, South Carolina, 1886 earthquake: Geology, v. 9, no. 3, p. 117-122.

Behrendt, J.C., Hamilton, R.M., Ackermann, H.D., Henry, V.J., and Bayer, K.C., 1983, Marine multichannel seismic-reflection evidence for Cenozoic faulting and deep crustal structure near Charleston, South Carolina, *in* Gohn, G.S., ed., Studies related to the Charleston, South Carolina, earthquake of 1886--Tectonics and seismicity: U.S. Geological Survey Professional Paper 1313-J, p. J1-J29.

Behrendt, J.C., and Klitgord, K.D., 1979, High resolution aeromagnetic anomaly map of the U.S. Atlantic continental margin: U.S. Geological Survey Geophysical Investigations Map GP-931, scale 1:1,000,000.

Behrendt, J.C., and Yuan, Annette, 1986, Strike slip on reactivated Triassic(?) basin boundary fault zones as sources of earthquakes near Charleston, S.C.: Earthquake Engineering Research Institute, Proceedings of the Third U.S. National Conference on Earthquake Engineering, v. 1, p. 43-54.

_____1987, The Helena Banks strike-slip (?) fault zone in the Charleston, South Carolina, earthquake area--Results from a marine, high-resolution, multichannel, seismic-reflection survey: Geological Society of America Bulletin, v. 98, no. 5, p. 591-601.

Bollinger, G.A., 1977, Reinterpretation of the intensity data for the 1886 Charleston, South Carolina, earthquake, *in* Rankin, D.W., ed., Studies related to the Charleston, South Carolina, earthquake of 1886--A preliminary report: U.S. Geological Survey Professional Paper 1028, p. 17-32.

Dewey, J.W., 1983, Relocation of instrumentally recorded pre-1974 earthquakes in the South Carolina region, *in* Gohn, G.S., ed., Studies related to the Charleston, South Carolina, earthquake of 1886--Tectonics and seismicity: U.S. Geological Survey Professional Paper 1313-Q, p. Q1-Q9.

_____1985, A review of recent research on the seismotectonics of the southeastern seaboard and an evaluation of hypotheses on the source of the 1886 Charleston, South Carolina, earthquakes: Washington, D.C., U.S. Nuclear Regulatory Commission report NUREG/CR-4339, 44 p.

Dillon, W.P., Paull, C.K., Buffler, R.T., and Fail, J.P., 1979, Structure and development of the southeast Georgia embayment and northern Blake Plateau--Preliminary analysis, *in* Watkins, J.S., Montadert, Lucien, and Dickerson, P.W., eds., Geological and geophysical investigations of continental margins: American Association of Petroleum Geologists Memoir 29, p. 27-41.

Gohn, G.S., ed., 1983, Studies related to the Charleston, South Carolina, earthquake of 1886--Tectonics and seismicity: U.S. Geological Survey Professional Paper 1313, 314 p.

Gohn, G.S., Gottfried, David, Lanphere, M.A., and Higgins, B.B., 1978, Regional implications of Triassic or Jurassic age for basalt and sedimentary red beds in the South Carolina Coastal Plain Science, v. 202, no. 4370, p. 887-890.

Gohn, G.S., Higgins, B.B., Smith, C.C., and Owens, J.P., 1977, Lithostratigraphy of the deep corehole (Clubhouse Crossroads corehole 1) near Charleston, South Carolina, *in* Rankin, D.W., ed., Studies related to the Charleston, South Carolina, earthquake of 1886--A preliminary report: U.S. Geological Survey Professional Paper 1028, p. 59-70.

Gottfried, David, Annell, C.S., and Byerly, G.R., 1983, Geochemistry and tectonic significance of subsurface basalts near Charleston, South Carolina: Clubhouse Crossroads test holes #2 and #3, *in* Gohn, G.S., ed., Studies related to the Charleston, South Carolina, earthquake of 1886--Tectonics and seismicity: U.S. Geological Survey Professional Paper 1313-A, p. A1-A19.

Gottfried, David, Annell, C.S., and Schwarz, L.J., 1977, Geochemistry of subsurface basalt from the deep corehole (Clubhouse Crossroads corehole 1) near Charleston, South Carolina--Magma type and tectonic implications, *in* Rankin, D.W., ed., Studies related to the Charleston, South Carolina, earthquake of 1886--A preliminary report: U. S. Geological Survey Professional Paper 1028-G, p. 91-113.

Grow, J.A., Bowin, C.O., and Hutchinson, D.R., 1979, The gravity field of the U.S. Atlantic continental margin: Tectonophysics, v. 59, p. 27-52.

Hamilton, R.M., Behrendt, J.C., and Ackermann, H.D., 1983, Land multichannel seismic-reflection evidence for tectonic features near Charleston, South Carolina, *in* Gohn, G.S., ed., Studies related to the Charleston, South Carolina, earthquake of 1886--Tectonics and seismicity: U.S. Geological Survey Professional Paper 1313-I, p. I1-I18.

Klitgord, K.D., and Behrendt, J.C., 1977, Aeromagnetic anomaly map of the United States Atlantic continental margin: U.S. Geological Survey Miscellaneous Field Studies Map MF-913, scale 1:1,000,000.

_____1979, Basin structure of the U.S. Atlantic margin, *in* Watkins, J.S., Montadert, Lucien, and Dickerson, P.W., eds., Geological and geophysical investigations of continental margins: American Association of Petroleum Geologists Memoir 29, p. 85-112.

Lanphere, M.A., 1983, $^{40}Ar/^{39}Ar$ ages of basalt from Clubhouse Crossroads test hole #2, near Charleston, South Carolina, *in* Gohn, G.S., ed., Studies related to the Charleston, South Carolina, earthquake of 1886--Tectonics and seismicity: U.S. Geological Survey Professional Paper 1313-B, p. B1-B8.

Rankin, D.W., ed., 1977, Studies related to the Charleston, South Carolina, earthquake of 1886--A preliminary report: U.S. Geological Survey Professional Paper 1028, 304 p.

Schilt, F.S., Brown, L.D., Oliver, J.E., and Kaufman, Sidney, 1983, Subsurface structure near Charleston, South Carolina: Results of COCORP reflection profiling in the Atlantic Coastal Plain, *in* Gohn, G.S., ed., Studies related to the Charleston, South Carolina, earthquake of 1886--Tectonics and seismicity: U.S. Geological Survey Professional Paper 1313-H, p. H1-H19.

Schneider, R.R., Gohn, G.S., Force, L.M., and King, S.L., 1979, Lithologic log for a deep stratigraphic test hole, Clubhouse Crossroads No. 3, Dorchester County, South Carolina: U.S. Geological Survey Open-File Report 79-449, 23 p.

Tarr, A.C., and Rhea, Susan, 1983, Seismicity near Charleston, South Carolina, March 1973 to December 1979, *in* Gohn, G.S., ed., Studies related to the Charleston, South Carolina, earthquake of 1886--Tectonics and seismicity: U.S. Geological Survey Professional Paper 1313-R, p. R1-R17.

Yantis, B.R., Costain, J.K., and Ackermann, H.D., 1983, A reflection seismic study near Charleston, South Carolina, *in* Gohn, G.S., ed., Studies related to the Charleston, South Carolina, earthquake of 1886--Tectonics and seismicity: U.S. Geological Survey Professional Paper 1313-G, p. G1-G20.

Zoback, M.L., Nishenko, S.P., Richardson, R.M., Hasegawa, H.S., and Zoback, M.D., 1986, Mid-plate stress, deformation, and seismicity, *in* Vogt, P.R., and Tucholke, B.E., eds., The Western North Atlantic region--The Geology of North America: Geological Society of America, Decade of North American Geology Series Volume M, p. 297-312.

HIGH-RESOLUTION MULTICHANNEL SEISMIC-REFLECTION PROFILES ACROSS THE HELENA BANKS STRIKE-SLIP FAULT ZONE OFFSHORE OF THE CHARLESTON, SOUTH CAROLINA, EARTHQUAKE AREA

By
Annette Yuan and John C. Behrendt

1988

Manuscript approved for publication July 19, 1988

INTERIOR--GEOLOGICAL SURVEY, RESTON, VA--1988

For sale by U.S. Geological Survey Map Distribution, Box 25286, Federal Center, Denver, CO 80225